Spontaneous appearance of rocking localized current filaments in a nonequilibrium distributive system

F.-J. Niedernostheide, B. S. Kerner, and H.-G. Purwins
Institut für Angewandte Physik der Universität Münster, Corrensstrasse 2/4, 4400 Münster, Germany
(Received 5 August 1991; revised manuscript received 30 March 1992)

In a p^+-n^+-p-n^- device driven by a dc-voltage source via a load resistor we experimentally observe a sequence of transitions when the total current is increased. A first transition from a stationary spatially homogeneous low-current state to a stationary localized current-density filament is followed by a second transition into a spontaneously rocking current filament oscillating with a definite frequency around a fixed position in space. For large total currents a third transition occurs. The rocking current filament transforms into a traveling current filament oscillating between the edges of the sample. A two-layer model for the device is proposed. The physical mechanism and the conditions for the appearance of rocking and traveling current filaments are considered and generalized for a wide class of nonequilibrium systems.

I. INTRODUCTION

In various nonequilibrium homogeneous distributive media—such as plasmas and gases, superconductors, photoconductors, active nonlinear optical systems, semiconductors and semiconductor devices, chemical and biochemical reactions—self-organized and self-maintained localized nonequilibrum structures may appear. Some years ago such localized structures were observed as stable stationary current filaments in experiments, e.g., in thin GaAs films,[1,2] in gold compensated silicon pin diodes,[3] in gas discharge systems,[4–6] periodic electric networks[7,8] and reverse biased p-n junctions.[9] The properties of these structures, e.g., form, width, amplitude, etc., are only determined by the system parameters. General results, theoretical and experimental, concerning the investigations of such structures (also called autosolitons) have been summarized in Refs. 10 and 11.

In some kinds of nonequilibrium media, standing localized states are spontaneously transformed into pulsating, sometimes called breathing, states[10,12–16] when certain parameters reach critical values. The amplitude or the width of pulsating nonequilibrium regions changes, with a certain frequency periodically in time.[12] Pulsating current filaments have experimentally been observed in p-Ge (Ref. 17) and n-GaAs.[18]

In this paper we report in Sec. II on the experimental observation that a standing current filament in a p^+-n^+-p-n^- device becomes unstable at a certain critical value of the total current. Instead of the expected transition to a pulsating current filament, a rocking filament is observed: A well-defined region of high current density oscillates around a fixed position in space with a definite frequency, similar to the motion of a pendulum. For rather large values of the total current, a further transition from a rocking to a traveling motion can be observed. In Sec. III we present a two-layer model for the p^+-n^+-p-n^- device. A new physical mechanism is proposed to explain that, under certain conditions, pulsating current filaments, or, in a more general sense, pulsating localized structures are suppressed, and rocking localized structures develop instead.

II. EXPERIMENTAL OBSERVATION OF SPONTANEOUSLY ROCKING CURRENT FILAMENTS

A. Experimental setup

The matter of our experimental investigations are rocking current filaments in silicon p^+-n^+-p-n^- structures, which are prepared by diffusion processes and ion implantation. A weakly phosphorus doped ⟨111⟩ silicon wafer with an impurity concentration of about 1.3×10^{13} cm^{-3} is used as the basic material. In two successive diffusion steps, the p and n^+ layers are produced, using aluminum and phosphorus as doping materials. The maximum doping concentrations are about 2×10^{16} cm^{-3} for the p layer and 5×10^{19} cm^{-3} for the n^+ layer. The p^+ layer is formed by ion implantation of boron with a maximum concentration of 5×10^{20} cm^{-3}. The widths of the n^-, p, n^+, and p^+ layers are 794, 70, 12, and 0.5 μm, respectively. A thin aluminum layer is evaporated on both sides of the wafer to provide the device with electrical contacts. For experimental investigations, small samples with typical sizes of about $(l_x\times l_y\times l_z)$ $=(5\times0.878\times0.5)$ mm^3 are prepared. The four semiconductor surfaces are finally polished.

A streak camera system with an $S1$ cathode has been used to measure the current-density distribution, spatially and temporally resolved. By this camera especially the emitted infrared recombination radiation can be detected. Incident light on a certain point of the cathode generates electrons which are accelerated in a high electric field and multiplied in a microchannel plate. An additional perpendicular electric field increasing linearly in time generates a spatiotemporally resolved picture on a phosphorus screen. For a detailed description of the streak camera system, see, e.g., Ref. 19. In the investigated samples, the intensity of the emitted radiation is large, especially in the environment of the p-n junctions and the me-

 ©1992 The American Physical Society

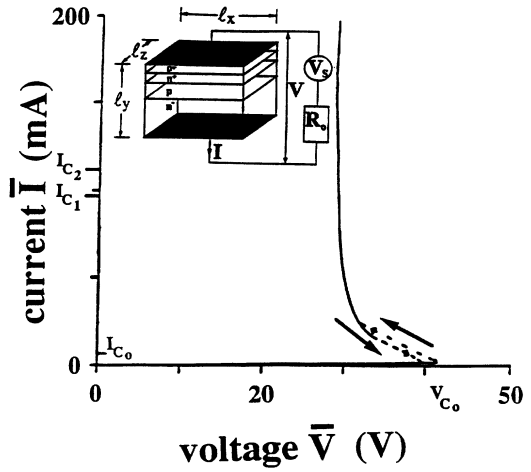

FIG. 1. Current-voltage characteristic $\bar{I}(\bar{V})$ of the p^+-n^+-p-n^- device. The inset shows the schematic structure of the device with the geometric dimensions $l_x=2.6$ nm, $l_y=0.88$ mm, and $l_z=0.7$ mm.

tallic contacts. The results presented in the following have been obtained by focusing a section of the $l_x l_y$ surface near the anode parallel to the contacts (Fig. 1) via a lens system to the streak camera.

B. Current-voltage characteristic and standing current filaments

The semiconductor device has been connected to a dc-voltage source via an external resistor R_0. Figure 1 shows the experimental setup and the total current-voltage characteristic $I(V)$ of the p^+-n^+-p-n^- device. In regions where the current or the voltage across the sample consists of a dc part and a superimposed ac part, we have used the average value of the corresponding variable. When increasing the supply voltage V_S, the voltage drop V across the sample increases until the critical voltage $V_{c0}\approx 42$ V is reached. The current density $j(x)$ is distributed homogeneously in the sample for total currents I in the interval $[0,I_{c0}]$. At the critical current I_{c0}, a standing current filament (Fig. 2) spontaneously appears connected with a discontinuity in the $I(V)$ characteristic. In almost all investigated samples, this current filament has been localized in a certain distance of one of the edges of the sample. From the detected radiation signal, a typical filament width of about 380 μm can be estimated.

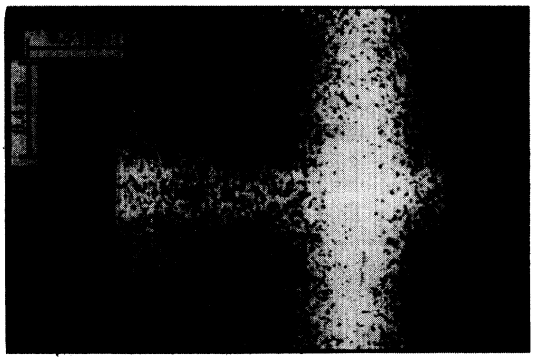

FIG. 2. Streak camera record of the emitted light density of a standing current filament for the current $I=91.3$ mA.

C. Spontaneous transition from a standing to a rocking current filament

If the total current in the system is increased, the current filament broadens a little and at a critical current value $I=I_{c1}$ (Fig. 1) the system undergoes a second transition: The standing filament becomes unstable and transforms to a rocking one [Fig. 3(a)], oscillating around a fixed position in space with the fundamental angular frequency $\omega=10\,300\ \mathrm{s}^{-1}$. This is accompanied by oscillations of the voltage across the sample with the amplitude V_{SS} and of the total current which have the same frequency ω [Fig. 3(b)]. The spatial amplitude l_r of the rocking filament is small compared to the length l_x of the sample. Further increase of the average current $\bar{I}=(1/T)\int_0^T I(t)dt$ with $T=2\pi/\omega$ causes an increase of the amplitude l_r, which, near the current I_{c1}, is proportional to the square root of the total average current [Figs. 4(a) and 4(c)]. We remark that the transition is connected only with small changes of the frequency values ω in the vicinity of the current I_{c1} [Fig. 4(b)].

D. Spontaneous transition from a rocking to a traveling current filament

By a further increase of the total current, a third transition occurs at I_{c2}. As can be seen from the streak cam-

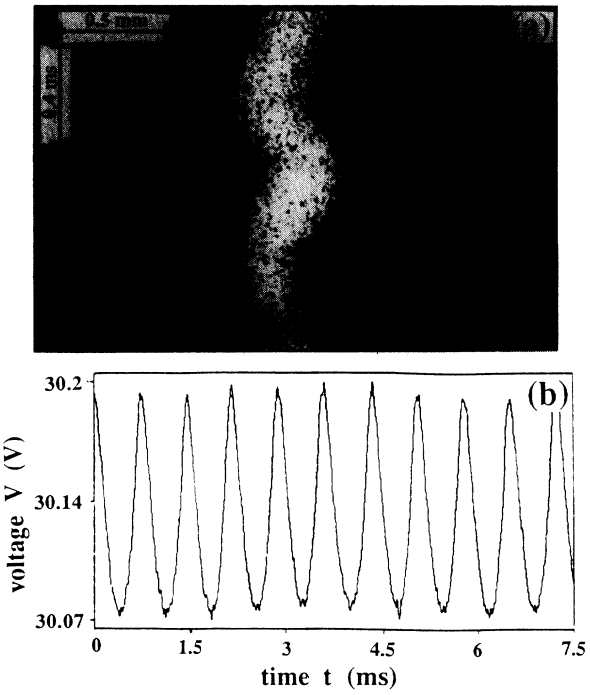

FIG. 3. Streak camera record of the emitted light density of a rocking current filament (a) and time series of the voltage drop V across the sample (b) for the average current $\bar{I}=106.5$ mA.

era record in Fig. 5(a), the small-amplitude oscillations around a fixed position in space are superimposed by oscillations of the current filament between the edges of the sample. Therefore, the amplitude of the rocking filament increases discontinuously at the critical point I_{c2}, while the frequency of the oscillation drops discontinuously. This behavior is reflected in the ac-voltage drop across the sample, the amplitude and frequency of which also increase or decrease discontinuously, respectively [Figs. 4(a) and 4(b) and Fig. 5(b)]. For a current $\bar{I} > I_{c2}$, the amplitude l_r is constant and equals nearly the sample length l_x, while the frequency increases with current $\bar{I}$ as shown in Fig. 4(b).

The transition from rocking to traveling current-density filaments becomes obvious in the $v = \dot{x}_c$ versus x_c diagram; v means the velocity and x_c the central position of the moving current filament. In the case of a rocking current filament, the velocity v changes from zero to v_{max} and back to zero nearly sinoidal [Fig. 6(a)]. Instead, a

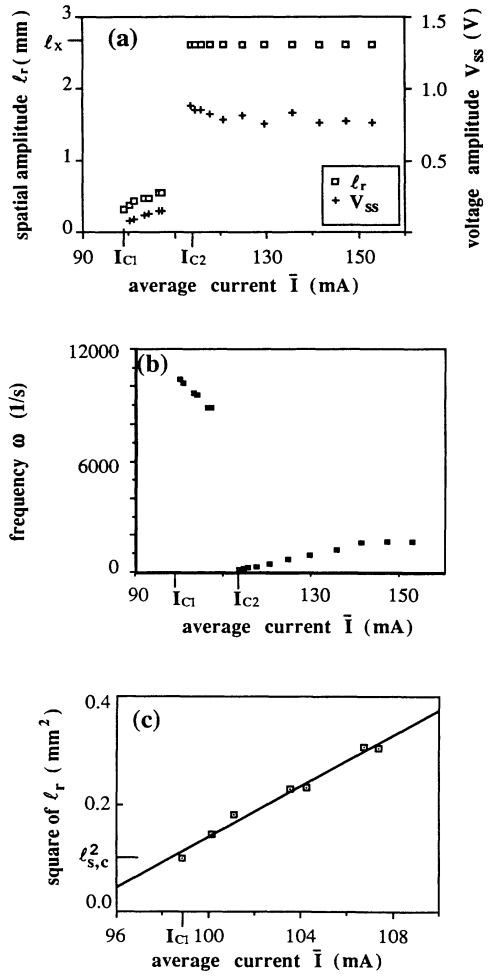

FIG. 4. Spatial amplitude l_r of the rocking current filament and amplitude V_{SS} of the voltage oscillations (a), and frequency ω of the rocking filament (b) as a function of the average current $\bar{I}$. In (c) the square of l_r as a function of $\bar{I}$ is drawn for $\bar{I}$ near to I_{c1}.

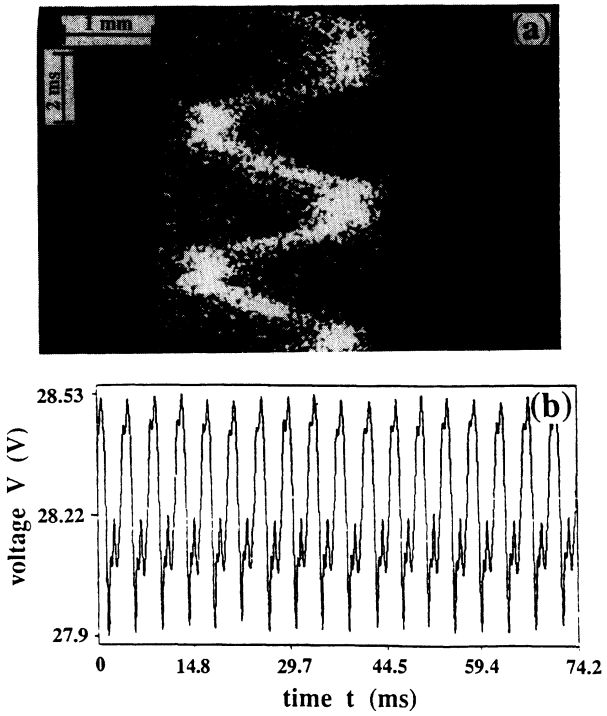

FIG. 5. Streak camera record of the emitted light density of a mainly traveling current filament (a) and time series of the voltage drop V across the sample (b) for the average current $\bar{I} = 146.6$ mA.

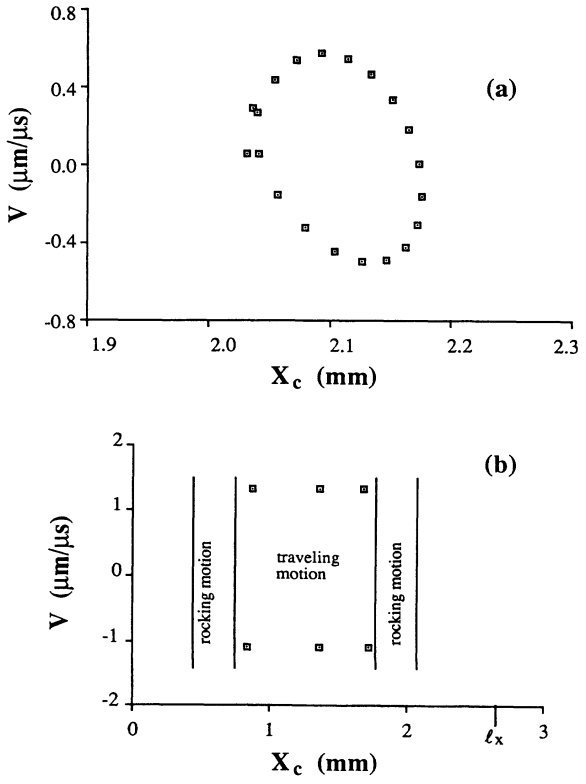

FIG. 6. Experimentally determined portrait of the phase space $v = \dot{x}_c$ vs x_c for a rocking (a) and a traveling (b) filament.

traveling current filament is characterized by space intervals in which the filament moves with a constant velocity up to the point where it reaches the edge of the sample [Fig. 6(b)]. Here the filament returns for a certain time period to a rocking motion before it travels back to the other edge. If the average current is large enough, the rocking motions near the edges vanish completely, leading to a pure traveling current filament.

E. The influence of the external resistor R_0

The presented results have been obtained by using a load resistor $R_0=610\ \Omega$ in the external electrical circuit. Under these circumstances, only small-current oscillations superimpose a dc current. The amplitude I_{SS} of these oscillations tends to zero when the value of the resistor increases to infinity [Fig. 7(a)], while the average current is kept constant and $\bar{I}\in[I_{c1},I_{c2}]$. On the other hand, the amplitude V_{SS} of the ac part of the voltage V and the spatial amplitude l_r are almost independent of R_0 as shown in Fig. 7(b). It is obvious that a pulsating current filament is connected with oscillations of the total current, whereas a pure rocking current filament does not change its width in time and therefore no oscillations of the total current can be expected. The experimental result that the amplitude I_{SS} grows with decreasing R_0 therefore indicates increasing pulsating components of the filament. However, the experiments show only rocking filaments, even at values of R_0 close to zero. This may be attributed to the resistance of the n^- layer of the device, which gives a contribution to an effective external resistor R_0.

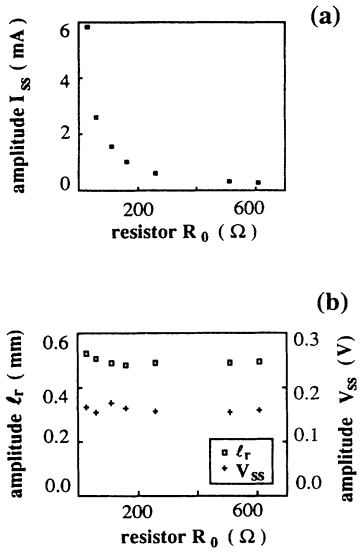

FIG. 7. Amplitude I_{SS} (a), spatial amplitude l_r and amplitude V_{SS} of the voltage oscillations across the sample (b) as a function of the external resistor R_0 for a rocking current filament. The average current $\bar{I}$ has been kept constant for all measurements.

III. THE MECHANISM LEADING TO THE APPEARANCE OF SPONTANEOUSLY ROCKING CURRENT FILAMENTS

A. A model for the investigated semiconductor sample

Let us consider the device (Fig. 8) composed of two parts: (i) a p^+-n^+-p transistor, and (ii) a forward-biased p-n^- junction.

The n^- layer is doped rather weakly (the donor concentration is about $1.35\times10^{13}\ \mathrm{cm}^{-3}$), such that the electron density is close to that of an intrinsic material. On this account, the injection of electrons from the n^- layer into the p layer and therefore into the first part of the device can be neglected in a first approximation, and the properties of this part are not influenced by the p-n^- junction. A consideration of the device based on two separated layers is therefore admissible.

In the first part of the device, the p^+-n^+-p transistor, the outermost p^+-n^+ junction is forward biased, whereas the inner n^+-p junction is reverse biased and blocks the current up to the voltage at which avalanche breakdown becomes important. Together with a positive-feedback mechanism by the outer p^+-n^+ junction, this p^+-n^+-p transistor exhibits an S-shaped current-voltage characteristic; i.e., the p^+-n^+-p transistor has a current-controlled negative resistance. If we restrict our considerations to only two space dimensions, the two parts of the device, namely the p^+-n^+-p transistor and the p-n^- junction, are coupled by the following relations:

$$j_{pnp}(x,y=0,t)=j_{pn}(x,y=0,t)\ , \tag{1a}$$

$$V(t)=V_j(x,t)+V_p(x,t)\ , \tag{1b}$$

where $j_{pnp}(x,y=0,t)$ and $j_{pn}(x,y=0,t)$ denote the current densities through the p^+-n^+-p structure and the p-n^- junction at the interface between the two parts of the device at $y=0$ [Figs. 8(a) and 8(b)]. $V_j(x,t)$, $V_p(x,t)$, and $V(t)$ are the voltage drops across the p^+-n^+-p structure, the p-n^- junction, and the whole device, respectively.

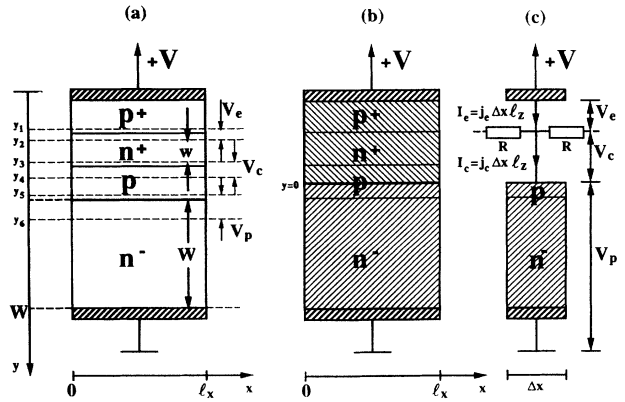

FIG. 8. Whole p^+-n^+-p-n^- device (a) and the proposed two-layer arrangement (b). The spreading of the emitter current (c) is determined by the base resistivity $R=\Delta x/(\sigma_b l_z w)$. y_1–y_6 mark the boundaries of the space-charge regions of the p-n junctions.

1. Description of the p^+-n^+-p transistor

In what follows, an equation for the emitter voltage V_e is derived, proceeding from the emitter and collector currents of the p^+-n^+-p-transistor. For the emitter current density $j_e(x,t)=j_e(x,y=y_2,t)$, a displacement current due to the emitter capacity C_e per unit square, a current arising from the diffusion of injected carriers and a recombination current are considered (see, e.g., Ref. 20):

$$j_e(x,t)=C_e\frac{\partial V_e(x,t)}{\partial t}+j_s\left[\exp\left[\frac{V_e(x,t)}{V_T}\right]-1\right]+j_r\left[\exp\left[\frac{V_e(x,t)}{2V_T}\right]-1\right]. \tag{2}$$

j_s and j_r denote saturation current densities of the forward-biased emitter-base diode, and the thermal voltage is defined by $V_T=kT/e$, with the elementary charge e the Boltzmann constant k, and the temperature T. The current densities j_s and j_r are explicitly given by

$$j_s=\frac{eD_{p,B}p_{n0,B}}{L_{p,B}}, \tag{3a}$$

$$j_r=\frac{ed_{\mathrm{EB}}}{2}\sigma v_{\mathrm{th}}N_t n_i, \tag{3b}$$

where $D_{p,B}$, $L_{p,B}$, and $p_{n0,B}$ are the diffusion constant, the diffusion length, and the equilibrium concentration of holes in the n^+ base, respectively. For j_r the usual model of Shockley-Read-Hall recombination is used. d_{EB} denotes the width of the space-charge region of the emitter-base junction, σ the electron and hole capture cross sections, which are assumed to be equal, v_{th} the thermal velocity of electrons and holes, N_t the trap density, and n_i the intrinsic density of carriers in silicon.

As is well known, the collector current density $j_c(x,t)=j_c(x,y=y_3,t)$ can be written as the sum of a displacement current, namely the collector saturation current, the transfer current of holes injected from the emitter, and a leakage current:

$$j_c(x,t)=C_c\frac{\partial V_c(x,t)}{\partial t}+Mj_{\mathrm{sc}}+M\beta j_s\left[\exp\left[\frac{V_e(x,t)}{V_T}\right]-1\right]+\frac{V_c(x,t)}{\rho_L}, \tag{4}$$

with the collector voltage drop V_c, the collector capacity C_c per unit square, and the multiplication factor M of the collector junction given by

$$M=\frac{1}{1-\left[\frac{V_c}{V_b}\right]^m}. \tag{5}$$

V_b is the common base breakdown voltage and m is a constant number. j_{sc} describes the saturation current density of the reverse-biased collector, β the base transport factor, and ρ_L the resistivity of the leakage. Taking into account the spreading of the current in the n^+ base, determined by the conductivity σ_b and the width w [Fig. 8(c)], the emitter and collector current are connected by

$$j_e(x,t)=j_c(x,t)+w\sigma_b\frac{\partial^2 V_e(x,t)}{\partial x^2}, \tag{6}$$

with the boundary conditions

$$\frac{\partial V_e(x=0,t)}{\partial x}=0, \quad \frac{\partial V_e(x=l_x,t)}{\partial x}=0. \tag{7}$$

Equations (2), (4), and (6), together with the boundary conditions (7), completely describe the behavior of the p^+-n^+-p transistor.

The reverse-biased collector has very often a rather small depletion layer capacity, leading to a fast relaxation of the collector voltage drop V_c. Neglecting the capacity in Eq. (4) and inserting it together with Eq. (2) into Eq. (6) yields

$$C_e\frac{\partial V_e}{\partial t}=w\sigma_b\frac{\partial^2 V_e}{\partial x^2}-(1-\beta M)j_s\left[\exp\left[\frac{V_e}{V_T}\right]-1\right]+Mj_{\mathrm{sc}}+\frac{V_i-V_e}{\rho_L}-j_r\left[\exp\left[\frac{V_e}{2V_T}\right]-1\right], \tag{8}$$

with $V_i(x,t)=V_e(x,t)+V_c(x,t)$ and $M=M(V_i-V_e)$ given by Eq. (5). The current density $j_{pnp}(x,y=0,t)$ is equal to the collector current density $j_c(x,t)$.

For this derivation, the injection of carriers in the transistor base was assumed to be not too large. In the case of high injection, the equation becomes more complex, but the important features for our consideration are contained already in the low injection model.

2. Description of the p-n^- junction

Let us consider now in more detail the electrical properties of the p-n^- junction. We make the following assumptions for simplification.

(i) The p-n^- junction is an ideal Shockley diode.

(ii) The n^- layer is weakly doped, therefore the injection of electrons from the n^- layer into the p layer can be neglected.

(iii) The width of the space-charge region and the width of the p region are neglected, i.e, $y_5=y_6=0$ [Fig. 8(a)]. The concentration of holes at the center of the p-n^- junction is therefore together with (i) given by

$$p(x,y=0,t)=p_{n0}\exp[V_p(x,y=0,t)/V_T]. \tag{9}$$

p_{n0} is the equilibrium concentration of holes in the n^- layer and V_p is the voltage drop across the p-n^- junction. Because of (i) and (ii), the current density j at the interface at $y=0$ is determined by the diffusion current of holes, leading to

$$\frac{\partial p(x,y=0,t)}{\partial y} = -\frac{j(x,y=0,t)}{eD_p} . \quad (10)$$

(iv) At the metallic contact $y = W$, surface recombination of holes with a surface recombination velocity s is assumed, so that the following boundary condition is valid:

$$\frac{\partial p(x,y=W,t)}{\partial y} = -s\frac{p(x,y=W,t)-p_{ns0}}{D_p} , \quad (11)$$

p_{ns0} is the hole equilibrium concentration at the metallic contact $y = W$.

(v) Low injection of holes in the n^- layer is assumed. Therefore, the rate of recombination of holes in the n^- layer can be approximated by $(p-p_{n0})/\tau_p$, where τ_p denotes the lifetime of holes in the n^- layer, and the hole current density due to electric fields can be neglected.[20] The hole current density j_p is then given by

$$j_p = -eD_p \nabla p(x,y,t) , \quad 0 \le y \le W , \quad 0 \le x \le l_x . \quad (12)$$

(vi) At the boundaries $x = 0$ and l_x we assume homogeneous Neumann boundary conditions

$$\frac{\partial p(x=0,y,t)}{\partial x} = 0 , \quad \frac{\partial p(x=l_x,y,t)}{\partial x} = 0 . \quad (13)$$

With these assumptions, the spatiotemporal development of the concentration of holes for $0 \le y \le W$ is determined by the following usual diffusion equation:

$$\frac{\partial p(x,y,t)}{\partial t} = D_p \left[\frac{\partial^2}{\partial x^2} + \frac{\partial^2}{\partial y^2} \right] p(x,y,t) - \frac{p(x,y,t)-p_{n0}}{\tau_p} \quad (14)$$

with the boundary conditions (10), (11), and (13).

In the following, for the sake of a qualitative understanding, we simplify the model equation (14) with the boundary conditions (10), (11), and (13). In this way the application of a general theory concerning the properties of localized solitary structures[10] becomes possible.

Because the main interest of our consideration concerns the distribution of holes in the x direction, it is useful to eliminate the dependence in the y direction by integrating Eq. (14) over the y axis. With $\bar{p}(x,t) = (1/W)\int_0^W p(x,y,t)\,dy$ and the surface recombination rate $1/\tau_s$ defined usually as (cf., e.g., Ref. 21)

$$\frac{1}{\tau_s} = -\frac{D_p \frac{\partial p(x,y=W,t)}{\partial y}}{\int_0^W [p(x,y,t)-p_{n0}]dy} = s\frac{p(x,y=W,t)-p_{ns0}}{\int_0^W [p(x,y,t)-p_{n0}]dy} , \quad (15)$$

the hole gradient at the boundary $y = W$ becomes

$$\frac{\partial p(x,y=W,t)}{\partial y} = -\frac{\bar{p}(x,t)-p_{n0}}{D_p \tau_s} W , \quad (16)$$

where W is the width of the n^- layer. Using Eqs. (10) and (16) after integration of Eq. (14),

$$\frac{\partial \bar{p}(x,t)}{\partial t} = D_p \frac{\partial^2 \bar{p}(x,t)}{\partial x^2} + \frac{j(x,y=0,t)}{eW} - \frac{\bar{p}(x,t)-p_{n0}}{\tau} \quad (17)$$

is obtained, with an effective lifetime τ defined by

$$\frac{1}{\tau} = \frac{1}{\tau_s} + \frac{1}{\tau_p}$$

and a generation term proportional to the current density $j(x,y=0,t)$ impressed from the p^+-n^+-p transistor. The boundary condition (13) for the average hole concentration concentration $\bar{p}(x,t)$ then becomes

$$\frac{\partial \bar{p}(x=0,t)}{\partial x} = 0 , \quad \frac{\partial \bar{p}(x=l_x,t)}{\partial x} = 0 . \quad (18)$$

We remark that in real devices the density of current may be so large that the assumption of low injection is not fulfilled. In the case of high injection, in addition to the voltage drop V_p across the p-n^- junction, a voltage drop across the n^- layer appears. Moreover, the holes injected from the p-n^- junction can accumulate near the n^--n^+ contact at the cathode, because this contact is a barrier for holes.

3. *Basic equations of the model*

By means of Eqs. (8) and (17), the p^+-n^+-p-n^- device is qualitatively described. Using the designations $\tau_e = C_e\rho_c$, $L = (D_p\tau)^{1/2}$, and $l = (w\sigma_b\rho_c)^{1/2}$,

$$q(V_e,V_i) = (1-\beta M) j_s \rho_c \left[\exp\left[\frac{V_e}{V_T} \right] - 1 \right] + j_r \rho_c \left[\exp\left[\frac{V_e}{2V_T} \right] - 1 \right] - M j_{sc} \rho_c - \frac{\rho_c}{\rho_L}(V_i - V_e) , \quad (19)$$

$$Q(V_e,V_i,V) = \frac{\tau}{eW} \left\{ M j_{sc} + \beta M j_s \left[\exp\left[\frac{V_e}{V_T} \right] - 1 \right] + \frac{V_i - V_e}{\rho_L} \right\} - [\bar{p}(V_i,V) - p_{n0}] , \quad (20)$$

and estimating the hole concentration $p(x,y=0,t)$ at the boundary of the space-charge region by the average hole concentration $\bar{p}(x,t)$, these equations can be rewritten in the following form:

$$\tau_e \frac{\partial V_e(x,t)}{\partial \tau} = l^2 \frac{\partial^2 V_e(x,t)}{\partial x^2} - q(V_e,V_i) , \quad (21a)$$

$$\tau \frac{\partial \bar{p}[V_i(x,t)]}{\partial t} = L^2 \frac{\partial^2 \bar{p}[V_i(x,t)]}{\partial x^2} + Q(V_e,V_i,V) , \quad (21b)$$

where the algebraic function $\bar{p}(V_i)$ is given by Eq. (9)

with $V_p = V - V_i$. ρ_c is the "characteristic" leakage resistivity which depends on the values of ρ_L and V_T/j_r.

The emitter voltage $V_e(x,t)$ is essentially determined by the function $q(V_e,V_i)$ with $\partial q/\partial V_e < 0$ for a certain range of the voltage V. In this range the injection of holes from the p^+ emitter leads to a positive feedback and to an autocatalytic increase of V_e. According to the exponential dependence of the emitter current density j_e on V_e, this positive feedback causes an increase of j_e. The physics of this autocatalytic process are based on the fact that holes injected from the emitter are multiplied in the collector region. In the operating mode of the avalanche transistor, the current density of the base is negative and the inequality $(1-\beta M)<0$ is fulfilled. If the value of the voltage drop V_i across the transistor is constant, this inequality means that the holes multiplied in the collector cause an electron base current from the collector which is large enough to induce an additional injection of holes from the emitter, and so on. Thus, the transistor part of the p^+-n^+-p-n^- device contains an autocatalytic process if V_i is constant. Because of this activating property of the transistor, the variable V_e may be called an activator. The time constant τ_e and the diffusion length l are the characteristic values over which V_e varies in time and space, respectively.

In the p^+-n^+-p-n^- device, the value of V_i is not constant due to interaction of the transistor with the p-n^- junction: The holes injected in the n^- layer increase the hole concentration $\bar{p}(x,t)$, and therefore the value of the voltage drop V_p across the p-n^- junction increases according to Eq. (9). Provided that the voltage drop $V(t)$ across the whole device is constant, the value of the voltage drop $V_i(x,t)=V(t)-V_p(x,t)$ across the transistor decreases if V_p increases. This inhibiting process in the p-n^- junction limits the autocatalytic process in the transistor part of the device. Because of this inhibiting property of the p-n^- junction, the variable V_i may be called an inhibitor. The time constant τ and the diffusion length L of holes spreading in the n^- layer determine the characteristic values over which V_i varies in time and space, respectively, according to Eqs. (9) and (21b). From Eqs. (20) and (21b) it is obvious that for each positive value of V_i and V_e the relation $\partial Q/\partial V_i > 0$ is fulfilled, indicating the fact that the voltage V_i works as an inhibitor.

From the external circuit we get a third equation for the voltage drop $V(t)$ across the whole device:

$$R_0 C_{\rm ex}\frac{\partial V(t)}{\partial t} = V_S - V - R_0\int_0^{l_x} j_c(V_e,V_i)dx \ , \qquad (22)$$

where V_S is the value of the applied voltage, $C_{\rm ex}$ the parasitic capacity parallel to the device, and R_0 the load resistor in the external circuit. The three equations (21a) (21b), and (22) for the voltages $V_e(x,t)$, $V_i(x,t)$, and $V(t)$ form a complete system of equations for the p^+-n^+-p-n^- device under consideration.

For $R_0=0$ and $R_0 C_{\rm ex} \ll \min(\tau_e,\tau)$ the values of V and V_S are equal, and the basic model equations are reduced to Eqs. (21a) and (21b) with $V=V_S$. A qualitative analysis of this system of equations for the ratios l/L or (and) τ_e/τ sufficiently small is possible using the theory from Ref. 10, if for a certain range of the parameter V the conditions

$$\partial Q/\partial V_i > 0 \ , \quad \partial q/\partial V_e < 0 \ , \qquad (23a)$$

$$\frac{\partial q}{\partial V_e}\frac{\partial Q}{\partial V_i} - \frac{\partial q}{\partial V_i}\frac{\partial Q}{\partial V_e} > 0 \qquad (23b)$$

are fulfilled. For the parameters of the p^+-n^+-p-n^- device, the value of the ratio l/L is rather small ($l/L<1$). This is due to the fact that l is determined by the spatial spreading of the base current in the thin n^+ base of the transistor and L depends on the spreading of holes in the thick n^- layer due to the ambipolar diffusion of electrons and holes. The value of τ_e/τ may be less than 1, too, because the effective lifetime τ of holes in the n^- layer can be much larger than the relaxation time τ_e of electrical processes in the transistor. From Ref. 10 it is known that, depending on the values of the ratios l/L and τ_e/τ, different kinds of localized structures can be expected for a constant value of V. Since the characteristic times as well as the characteristic lengths of the activator V_e, i.e., the current density through the transistor, and those of the inhibitor V_i, are different, a competition in time and space between these two variables appears. In Sec. III B a qualitative explanation based on this competition is given for the experimental phenomena presented in Sec. II of this paper.

B. Physics of standing localized current filaments

In this section we consider qualitatively the physical properties of current-density filaments in the proposed model. For that purpose it is useful to consider first the characteristic dependence of the device variables V_e and V_i for homogeneous distributions.

The current-voltage characteristic of the first part of the device, the p^+-n^+-p transistor, is according to Eq. (2) connected to the relation $V_e(V_i)$, because $j_e(V_e)$ is a monotonic function. As can be seen from Eq. (21a), the function $V_i(V_e)$ can be obtained from the equation $q(V_e,V_i)=0$. For the following set of parameters $V_i(V_e)$ is depicted in Fig. 9(a): $j_{\rm sc}=2\times10^{-8}$ A/cm^2, $j_s=1.5\times10^{-11}$ A/cm^2, $j_r=3\times10^{-7}$ A/cm^2, $T=300$ K, $\beta=0.6$, $V_b=42$ V, $m=3$, $W=600$ μm, $\rho_L=4\times10^4$ Ω cm^2. Due to the exponential dependence of j_e on V_e, small variations of V_e result in large variations of j_e, and due to the relation $V_e(V_i)$ the current-voltage characteristic of the p^+-n^+-p transistor becomes highly nonlinear with a region of negative differential resistance [Fig. 9(b)].

It is well known[22,23] that in such devices "nonlocalized" current-density filaments can appear. The characteristic length over which the current density changes in space is determined by the value of l (Fig. 10). The term nonlocalized means that the appearance of the current filament is accompanied by a change of the current density $j(x,t)$ through the transistor in the whole x range when compared with the homogeneous current distribution. The existence of the current filament is linked with the positive-feedback mechanism caused by the avalanche breakdown in the collector and the injection of holes

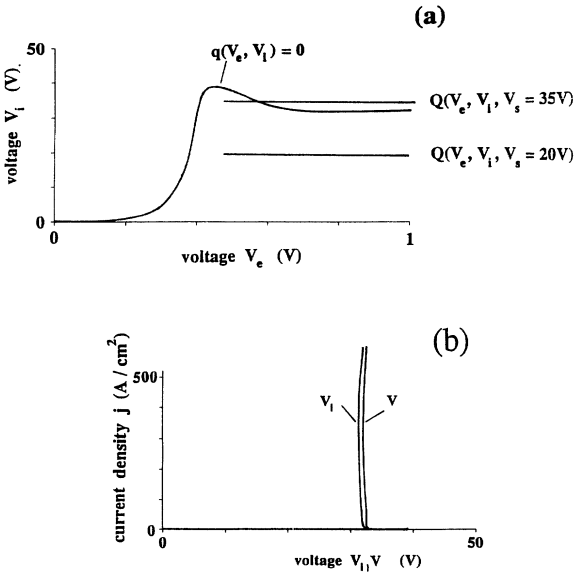

FIG. 9. Dependence of the transistor voltage V_i on the emitter voltage V_e for $q(V_e,V_i)=0$ and $Q(V_e,V_i,V_S)=0$ (a). The calculated current-voltage characteristics in (b) refer to the transistor part $[j(V_i)]$ and the whole p^+-n^+-p-n^- device $[j(V)]$ for a homogeneous current distribution.

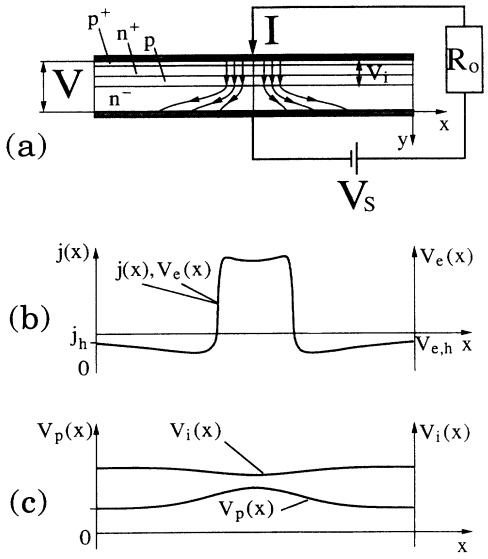

FIG. 11. Schematic arrangement of the p^+-n^+-p-n^- device (a) with a localized current filament (b) that can develop because of the spreading of holes in the n^- layer. The spreading leads to the long-range distribution of the voltages V_p and $V_i = V - V_p$ (c).

from the emitter, as considered in Sec. III A 3.

The whole device consists not only of the transistor, but also of the p-n^- junction. For this reason, in the p^+-n^+-p-n^- device, "localized" current filaments appear instead of well-known nonlocalized current filaments (Fig. 11). In this case, far from the localized current filament, the current density is equal to the homogeneous density $j=j_h$, in contrast to the nonlocalized case. In regions where the value of the current density corresponds to the value j_h of the homogeneous distribution, the system does not know about the existence of the localized high-current region.

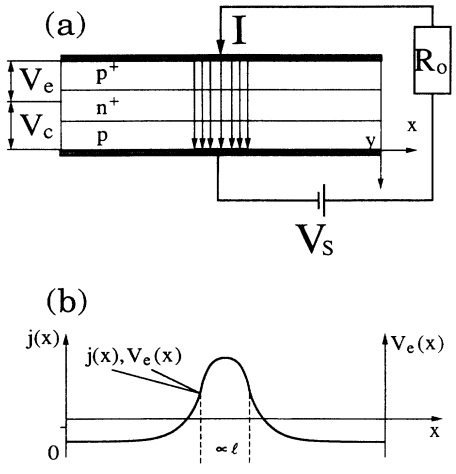

FIG. 10. Schematic arrangement of the p^+-n^+-p transistor (a) with a nonlocalized current filament (b). The distributions of the emitter current $j_e(x)$ and the emitter voltage $V_e(x)$ differ only by their scaling.

The physical reason for the appearance of localized current filaments can be qualitatively explained as follows: Holes that are injected from the transistor into the n^- layer diffuse in this layer. Because in the center of the filament the injection of holes is many times larger than in the vicinity of the filament, holes diffuse not only to the cathode but also along the x direction in the thick n^- layer. This broadening of the region with high hole concentration in the n^- layer [Fig. 11(a)] causes a corresponding broad distribution of the voltage drop $V_p(x,t)$ across the p-n^- junction. According to Eq. (1), the voltage drop $V_i(x,t)$ across the transistor in this case depends on the spatial x coordinate and reaches in a certain distance from the center of the current filament, a value corresponding to a homogeneous state. This distance is determined by the value of L, which in turn is determined by the diffusion length of holes in the n^- region. Thus the characteristic width of a localized current filament is determined by L. We remark that the lifetime τ_p of holes in the n^- region of our device is about 100 μs. The value of $L=(D_p\tau)^{1/2}$ is therefore about 350 μm for $D_p=12.5$ cm^2/s if τ is approximated by τ_p, and is of the order of the observed width of the filament.

The existence of a localized current filament [Figs. 11(b) and 11(c)] is linked with the fact that the value of the voltage drop V_i across the transistor locally decreases and suppresses a further increase of the current density. For this reason, the maximal current density in the filament is limited. If the condition $L > l$ is fulfilled, the spreading of holes in the n^- layer leads to a less-pronounced decrease of V_i in comparison with the homogeneous case. In this case, the decrease of V_i in the center of the filament is smaller and therefore cannot prevent the generation of a localized high-current-density

region. Thus a localized filament exists due to the competition of the positive feedback in the transistor and the negative feedback in the p-n^- junction if $L > l$. The competition also determines the size l_s of such a localized state. The boundaries of this state are characterized by sharply changing current densities [Fig. 11(b)] due to the large positive feedback in the transistor. These boundaries may be called "walls" of the localized current filament.

For the device under consideration, the dependence of V_i on V_e resulting from the equation $q(V_e, V_i)=0$ is not monotonic (Fig. 9) but is N shaped, corresponding to an S-shaped $V_e(V_i)$ characteristic. On the contrary, the dependence of V_i on V_e derived from $Q(V_e, V_i)=0$ is monotonic. Furthermore, the inequality $l/L \ll 1$ can be fulfilled for the device if ρ_c is approximated by $(2V_T/j_r)\exp(-V_e/2V_T)$ and V_e is sufficiently large. Therefore, the results for the stability and properties of autosolitons in active distributed systems from Ref. 10 can be applied tentatively for further qualitative considerations concerning the behavior of localized current filaments in the device.

C. Physics of the transition from standing to pulsating localized current filaments

Possible transitions from standing to other kinds of localized current filaments are predictable from qualitative considerations of the stability of standing localized current filaments. In the case of stable localized structures, the growth of critical current fluctuations that are localized in the current filament walls is damped by the inhibitor V_i. There are mainly two critical fluctuations of the activator δV_{e0} and δV_{e1} corresponding to current-density fluctuations δj_0 and δj_1 [Figs. 12(b) and 12(c)]. They induce a corresponding alteration δV_i, which in turn has a damping influence on the growth of the fluctuations δj. From an analysis in Ref. 10, it is known that the most destabilizing perturbation for a localized current filament is the symmetric fluctuation δj_0, which modifies the width l_s of a filament. If the characteristic time of temporal changes of the voltage V_i (inhibitor) is much larger than that of the current density $j=j_e$ (activator), i.e., $\tau_e/\tau \ll 1$, the critical fluctuation of the activator cannot instantly be suppressed by the inhibitor. Hence the amplitude δj_0 [Fig. 12(b)] of the activator fluctuation

$$\delta j(x,t)=\delta j_0(x)\cos(\omega_c t) \tag{24}$$

increases, and the fluctuation has an intrinsic frequency ω_c, $\tau^1 < \omega_c < \tau_e^{-1}$, with[10]

$$\omega_c = \left[\frac{l}{L}\frac{1}{\tau_e \tau}\right]^{1/2} . \tag{25}$$

The increasing fluctuation $\delta j(x,t)$ causes wall oscillations of the localized current filament. These wall oscillations are in antiphase, and therefore a transition from a standing to a pulsating localized current filament takes place [Fig. 12(d)].

From Refs. 24 and 25, it is known that, besides wall oscillations in antiphase, oscillations in phase can also appear. In systems with a parameter V that is independent on the total current [cf. Eq. (22)] oscillations in phase take place only in a secondary transition as a rule, and therefore only wall oscillations in antiphase can be expected to appear spontaneously. In the following we shall show that, under certain conditions, the transition from a standing to a pulsating current filament is suppressed, and a spontaneous transition to a rocking one [Fig. 12(e)] takes place instead.

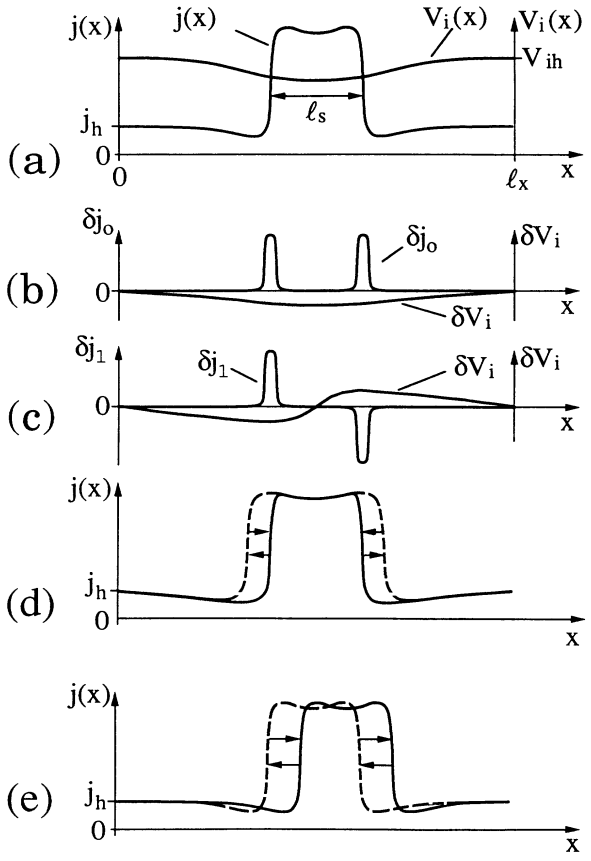

FIG. 12. Spatial stable stationary distribution of the current density (activator) and the voltage V_i (inhibitor) (a). The symmetric (b) and antisymmetric (c) critical fluctuations δj_0 and δj_1 of the current density with the corresponding fluctuations δV_i of the transistor voltage lead to pulsating (d) and rocking (e) filaments, respectively. The solid and dashed lines mark the two extreme positions of the filament.

D. Physics of the spontaneous transition from standing to rocking localized current filaments

In this section we explain why in our experimental investigations not a transition from a standing to a pulsating current filament, but instead a transition to a rocking localized current filament spontaneously appears at some critical value of the total current I through the device.

In order to observe the transition from a standing to a pulsating localized current filament, it is necessary that the critical symmetric fluctuation δj_0 [Fig. 12(b)] can grow. Since the perturbation δj_0 is symmetric to the center of the localized current filament, it changes the

width of the current filament and thereby the total current:

$$I=l_z\int_0^{l_x} j(x)dx \ . \tag{26}$$

l_x and l_z denote the size of the system in the x and z directions. Therefore, δj_0 can only be effective if the load resistor R_0 in the external circuit is sufficiently small or even zero. For increasing values of the external resistor R_0, the fluctuations δj_0 are more and more damped and finally completely suppressed at a certain critical value $R_{0,c}$. In the limit case of a current source, i.e., $R_0=\infty$, it is evident that the total current I is constant and symmetric fluctuations such as δj_0 cannot appear. For the above considered cases with $j=j_e(V_e)$ and $\partial j_e/\partial V_e>0$ we obtain

$$\delta I=l_z\int_0^{l_x}\delta j(V_e)dx=l_z\int_0^{l_x}\frac{\partial j}{\partial V_e}\delta V_e(x)dx=0 \ , \tag{27}$$

and thereby $\delta V_{e0}=\delta j_0=0$. In contrast to this, the fluctuation $\delta j=\delta j_1$ [Fig. 12(c)] leading to a rocking current filament [Fig. 12(e)] can grow if $R_0=\infty$, since δj_1 is antisymmetric and therefore condition (27) is fulfilled, even for $\delta j_1\neq 0$. The condition under which such antisymmetric fluctuation increase is well known from the general theory of autosolitons[10] and is given by

$$\lambda_1+\frac{\tau_e}{\tau}\mu_1<0 \ , \tag{28}$$

where

$$\lambda_1=-\begin{cases}\left[l/L\right]^2(l_s/l) \ , & l_s<L\\ l/L \ , & l_s>L\end{cases} \tag{29}$$

is the increment of the growing fluctuation δj_1 if the inhibitor fluctuation δV_i is assumed to be zero. $\mu_1>0$ is the decrement of the inhibitor fluctuation δV_{i1} if the activator fluctuation δj_1 is assumed to be zero. The term $(\tau_e/\tau)\mu_1$ describes the damping effect by changing the inhibitor density. On the condition that

$$\tau_e/\tau<l/L\ll 1 \tag{30}$$

is valid, we obtain from Eqs. (28) and (29) the existence of a critical width $l_{s,c}$ of a current-density filament, or, more general, of an autosoliton. This width $l_{s,c}$ is given by

$$l_{s,c}=L\frac{\tau_e}{\tau}\frac{L}{l} \ . \tag{31}$$

If the width of a standing localized current filament exceeds the critical value $l_{s,c}$ and current fluctuations in the external circuit are suppressed by using a current source, the standing localized current filament becomes unstable and transforms into a rocking one, because

$$\delta j(x,t)=\delta j_1(x)\cos(\omega_{c1}t) \tag{32}$$

describes a perturbation leading to an oscillation of a localized current filament with the frequency $\omega_{c1}\approx\omega_c$ [cf. Eq. (25)] around a certain spatial position. Since any value of the total current corresponds to a definite value of the filament width l_s, the spontaneous transition from a standing to a rocking filament occurs if the total current I exceeds a certain value I_c corresponding to the critical width $l_{s,c}$. Thus a rocking localized current filament appears instead of a pulsating one if the external resistor as well as the total current exceed a certain critical value.

As in many other cases, two types of spontaneous transitions from standing to rocking localized current filaments can be distinguished. The first type is characterized by a transition from a standing to a rocking current filament connected with a discontinuous rise of the amplitude of the rocking current filament. The frequency of such a rocking current filament may be much less than ω_c because the oscillation may be of a relaxation type with two different characteristic times of the activator (V_e or j_e) and the inhibitor (V_i). In the second case, the spatial amplitude of the rocking current filament increases smoothly, with an enlargement of the total current I from zero at $I=I_{c1}$ with a frequency near ω_c. This is the type of transition observed experimentally (Fig. 3). Near the critical current I_{c1} a well-known scaling law between the spatial amplitude l_r of the rocking motion and the total average current could be found: $l_r\sim(\bar{I})^{1/2}$.

E. Traveling localized current filaments

A traveling current filament is moving with a constant velocity that depends only on the parameters of the device. In contrast, the velocity of a rocking current filament changes in space and reaches the maximal value in the spatial center of the rocking motion. It becomes zero at the extreme points of the spatial motion. If the system is periodically closed, e.g., as a ring, we can expect a spontaneous transition from a rocking to a traveling motion.

In experiment, the transition from a rocking to a traveling current filament has been found, when the total current exceeds the critical current I_{c2}, as can be seen from Fig. 5. The concrete geometrical form of the device under consideration is a linear setup as a stripe (Fig. 1). Therefore, the filament has to approach one of the semiconductor surfaces of the sample. We observed experimentally a new effect, namely, the repelling of the filament at the surface. By this, a filament oscillating between the two edges results. The velocity of this localized current filament in a certain distance of the surface is almost constant [cf. Fig. 6(b)] in the whole sample, indicating a traveling current filament. Only if the filament reaches one of the surfaces can a sharp change of the velocity v to zero and a change of the sign of the velocity be observed. During the repelling period, the filament characterized by the lightening region does not reach the semiconductor surface [Fig. 5(a)]. This experimental observation can be explained using the general properties of traveling autosolitons in active systems for which the inequality (30) is valid.

From the theory of traveling autosolitons in infinite ex-

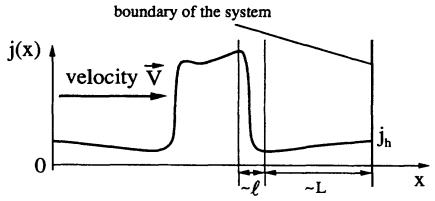

FIG. 13. Schematic distribution of a traveling current filament near the boundary.

tended systems, described by two nonlinear equations for an activator and an inhibitor without global inhibition, it is known[10] that, in front of the first wall of the traveling autosoliton, a diffusion precursor of the inhibiting component V_i exists. The diffusion precursor leads to a refractory region of order L in size. In this refractory region, the current density changes smoothly from $j_{\min}$ to j_h (Fig. 13). The diffusion precursor in front of the traveling current filament acts as a feeler of the filament. By means of this feeler, the filament is able to notice the semiconductor surface if it has approached the surface to a distance L. The velocity of the filament begins to decrease, and the repelling mechanism starts. For this reason, the front wall of the traveling current filament does not reach the surface and repels in a certain distance of it [Fig. 5(a)].

The repelling mechanism at the boundary in a system in which Eq. (30) is valid is of the same nature as the repelling due to collisions of current filaments in extended systems as observed, e.g., in gas-discharge systems[26] and as predicted in Ref. 10. We remark that the repelling effect of traveling current filaments at the boundary of the system or at another current filament is quite different from the well-known behavior of traveling in many active system described by models of the FitzHugh-Nagumo (FHN) type (see, e.g., Ref. 27). In this case, the collision of two current filaments leads to an annihilation; a repulsion is impossible. This annihilation effect in the FHN case is caused by the short inhibitor length corresponding to a missing feeler of the filament.

IV. ABOUT ROCKING FIELD DOMAINS

We can extend the proposed mechanism concerning the appearance of rocking localized structures to systems that allow the existence of localized electric-field domains. Standing localized domains are well known in experiments, e.g., in composite superconductors.[28] Here the characteristic time scale on which the activator changes corresponds to that of the temperature of the lattice, and the time constant referring to the inhibitor is determined by the inductance of the system. If in such a system the ratio of the characteristic time constants of the activator and the inhibitor is rather small and the external resistor R_0 is smaller than a certain critical value, the standing electric domain becomes unstable with respect to a rocking, not to a pulsating, domain. In the limiting case of $R_0=0$ and when using a voltage source in the external circuit, the voltage drop V across the sample,

$$V=\int_0^{l_x} E(x)dx \ , \tag{33}$$

is constant; therefore, it follows that

$$\delta V=\int_0^{l_x} \delta E(x)dx=0 \ . \tag{34}$$

From Eq. (34) it is obvious that only antisymmetric fluctuations δE_1 can arise, and consequently only rocking, not pulsating, electric domains can appear.

V. CONCLUSION

In this paper the experimentally observed behavior of a p^+-n^+-p-n^- semiconductor device has been presented. Transitions between standing, rocking, and traveling localized current filaments occur. The proposed two-layer model leads to a two-component reaction-diffusion equation in which voltage drops across p-n junctions correspond to an activating and an inhibiting component. It could be shown that due to the properties of a global coupling, which has been realized by an external load resistor, the appearance of pulsating filaments can be suppressed and rocking filaments become favored. We conclude that the scenario reported in this paper and in particular the appearance of rocking and traveling current filaments as well as the observed repelling mechanism is not restricted to the investigated semiconductor structures, in which we experimentally discovered these phenomena. Such a behavior can be expected for many other nonequilibrium distributive systems in which localized structures can appear.

ACKNOWLEDGMENTS

We would like to thank Dr. H.-J. Schulze from the Siemens AG, Munich for preparation of the semiconductor samples, and we gratefully acknowledge the financial support of the Stiftung Volkswagenwerk.

[1]B. S. Kerner and V. F. Sinkevich, Pis'ma Zh. Eksp. Teor. Fiz. **36**, 359 (1982) [JETP Lett. **36**, 436 (1982)].

[2]K. M. Mayer, J. Parisi, and R. P. Huebener, Z. Phys. B **71**, 171 (1988).

[3]D. Jäger, H. Baumann, and R. Symanczyk, Phys. Lett. A **117**, 141 (1986).

[4]Ch. Radehaus, T. Dirksmeyer, H. Willebrand, and H.-G. Purwins, Phys. Lett. A **125**, 92 (1987).

[5]H.-G. Purwins, G. Klempt, and J. Berkemeier, in *Festkörperprobleme (Advances in Solid State Physics)*, edited by P. Grosse (Vieweg, Braunschweig, 1987), Vol. 27, p. 27.

[6]H. Willebrand, C. Radehaus, F.-J. Niedernostheide, R. Dohmen, and H.-G. Purwins, Phys. Lett. A **149**, 131 (1990).

[7]J. Berkemeier, T. Dirksmeyer, G. Klempt, and H. G. Purwins, Z. Phys. B **65**, 255 (1986).

[8]H.-G. Purwins and Ch. Radehaus, *Neural and Synergetic Com-*

puters, edited by H. Haken (Springer, Berlin, 1988).
[9]B. S. Kerner, B. P. Litvin, and V. I. Sankin, Pis'ma Zh. Tekh. Fiz. **13**, 819 (1987) [Sov. Tech. Phys. Lett. **13**, 342 (1987)].
[10]B. S. Kerner and V. V. Osipov, Usp. Fiz. Nauk **157**, 201 (1989) [Sov. Phys. Usp. **32**, 101 (1989)].
[11]B. S. Kerner and V. V. Osipov, Usp. Fiz. Nauk **160**, 1 (1990) [Sov. Phys. Usp. **33**, 679 (1990)].
[12]B. S. Kerner and V. V. Osipov, Zh. Eksp. Teor. Fiz. **83**, 2201 (1982) [Sov. Phys. JETP **56**, 1275 (1982)].
[13]Y. Nishiura and M. Mimura, SIAM J. Appl. Math. **49**, 481 (1989).
[14]S. Koga and Y. Kuramoto, Prog. Theor. Phys. **63**, 106 (1980).
[15]H. Willebrand, F.-J. Niedernostheide, R. Dohmen, and H.-G. Purwins, in *Oscillations and Morphogenesis,* edited by L. Rensing, (Dekker, New York, 1992).
[16]B. S. Kerner and V. V. Osipov, Mikroelektronika **6**, 337 (1977).
[17]U. Rau, W. Clauss, A. Kittel, M. Lehr, M. Bayerbach, J. Parisi, J. Peinke, and R. P. Heubener, Phys. Rev. B **43**, 2255 (1991).
[18]A. Brandl, M. Völcker, and W. Prettl, Solid State Commun. **72**, 847 (1989); A. Brandl and W. Prettl, in *Festkörperprobleme (Advances in Solid State Physics),* edited by U. Rössler (Vieweg, Braunschweig, 1990), Vol. 30, p. 371.
[19]Y. Tsuchiya, IEEE J. Quantum Electron. **QE-20**, 1516 (1984).
[20]S. M. Sze, *Physics of Semiconductor Devices,* 2nd ed. (Wiley, New York, 1981).
[21]J. W. Orton and P. Blood, in *Techniques of Physics* edited by N. H. March (Academic, London, 1990), Vol. 13.
[22]A. V. Volkov and Sh. M. Kogan, Usp. Fiz. Nauk **96**, 633 (1968) [Sov. Phys. Usp. **11**, 881 (1969).
[23]E. Schöll, *Nonequilibrium Phase Transitions in Semiconductors* (Springer, Berlin, 1987).
[24]B. S. Kerner and V V. Osipov, Mikroelecktronika **12**, 512 (1983).
[25]B. S. Kerner and V. V. Osipov, Zh. Eksp. Teor. Fiz. **89**, 589 (1985) [Sov. Phys. JETP **62**, 337 (1985)].
[26]H. Willebrand, T. Hünteler, F.-J. Niedernostheide, R. Dohmen, and H.-G. Purwins, Phys. Rev. A **45**, 8766 (1992).
[27]See, e.g., R. FitzHugh, Biophys. J. **1**, 445 (1961); I. Nagumo, S. Arimoto, and S. Yoshizawa, Proc. IRE **50**, 2061 (1962); A. Mikhailov, in *Foundations of Synergetics I,* Springer Series of Synergetics Vol. 51 (Springer, Berlin, 1990).
[28]A. V. Gurevich and R. G. Mints, Rev. Mod. Phys. **59**, 941 (1987).

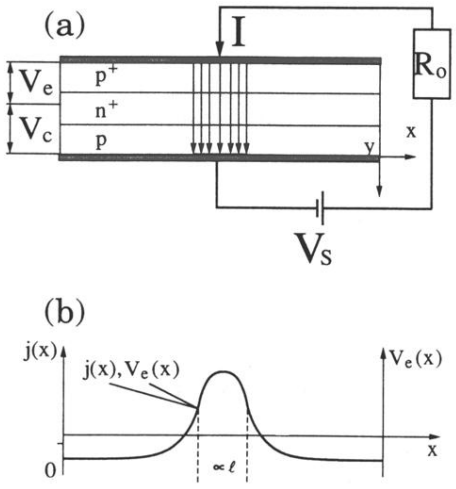

FIG. 10. Schematic arrangement of the p^+-n^+-p transistor (a) with a nonlocalized current filament (b). The distributions of the emitter current $j_e(x)$ and the emitter voltage $V_e(x)$ differ only by their scaling.

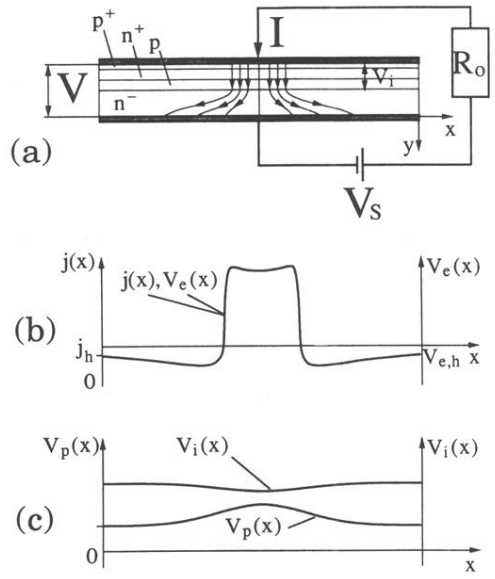

FIG. 11. Schematic arrangement of the p^+-n^+-p-n^- device (a) with a localized current filament (b) that can develop because of the spreading of holes in the n^- layer. The spreading leads to the long-range distribution of the voltages V_p and $V_i = V - V_p$ (c).

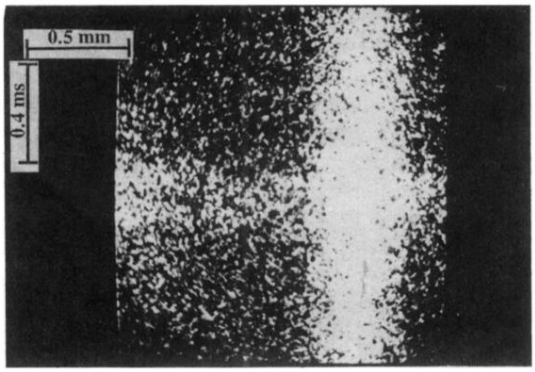

FIG. 2. Streak camera record of the emitted light density of a standing current filament for the current $I = 91.3$ mA.

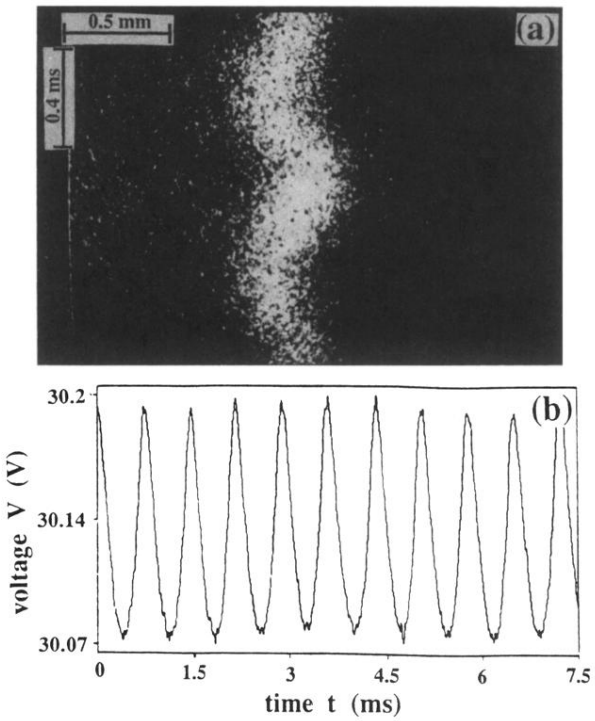

FIG. 3. Streak camera record of the emitted light density of a rocking current filament (a) and time series of the voltage drop V across the sample (b) for the average current $\bar{I}=106.5$ mA.

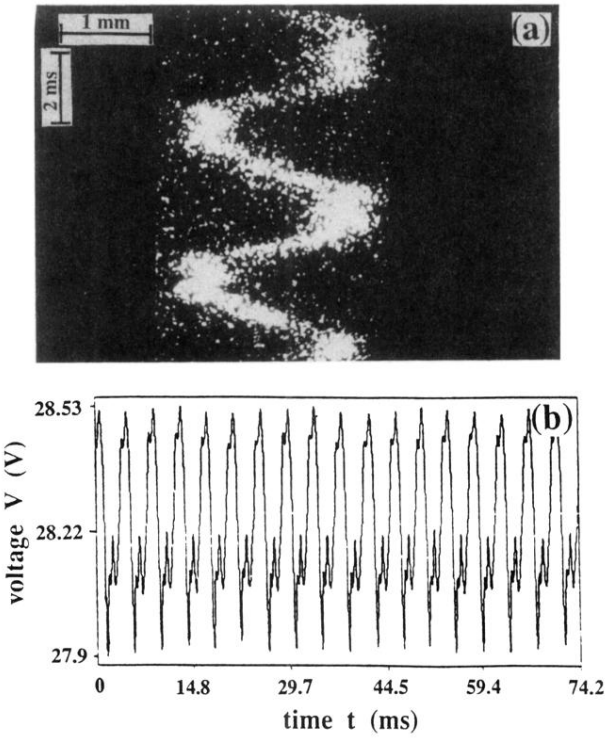

FIG. 5. Streak camera record of the emitted light density of a mainly traveling current filament (a) and time series of the voltage drop V across the sample (b) for the average current $\bar{I}=146.6$ mA.